DOI:
10.1063/1.4961054

Document Version
Publisher's PDF, also known as Version of record

AIP | Applied Physics Letters

Picosecond wide-field time-correlated single photon counting fluorescence microscopy with a delay line anode detector

Liisa M. Hirvonen, Wolfgang Becker, James Milnes, Thomas Conneely, Stefan Smietana, Alix Le Marois, Ottmar Jagutzki, and Klaus Suhling

Citation: Applied Physics Letters **109**, 071101 (2016); doi: 10.1063/1.4961054
View online: http://dx.doi.org/10.1063/1.4961054
View Table of Contents: http://scitation.aip.org/content/aip/journal/apl/109/7?ver=pdfcov
Published by the AIP Publishing

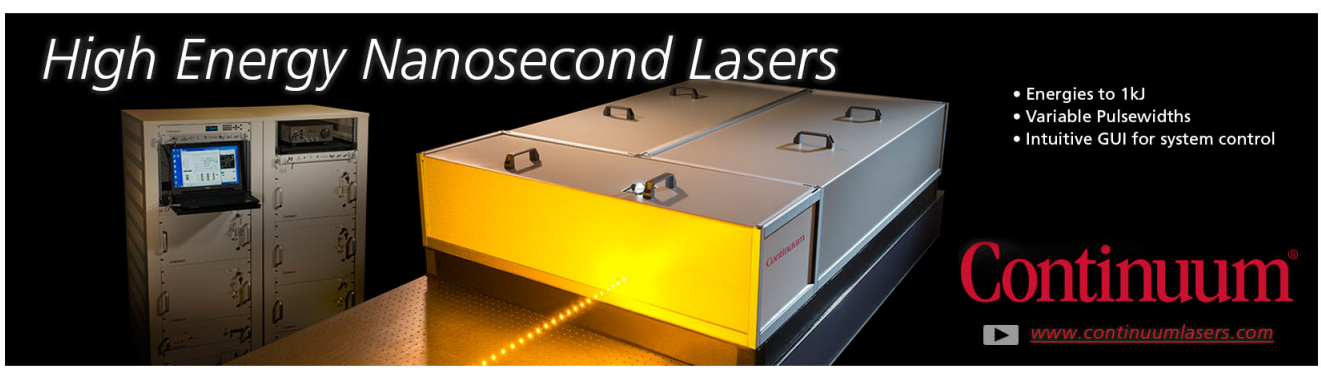

Picosecond wide-field time-correlated single photon counting fluorescence microscopy with a delay line anode detector

Liisa M. Hirvonen,[1] Wolfgang Becker,[2] James Milnes,[3] Thomas Conneely,[3] Stefan Smietana,[2] Alix Le Marois,[1] Ottmar Jagutzki,[4] and Klaus Suhling[1,a)]
[1]*Department of Physics, King's College London, Strand, London WC2R 2LS, United Kingdom*
[2]*Becker & Hickl GmbH, Nahmitzer Damm 30, 12277 Berlin, Germany*
[3]*Photek Ltd., 26 Castleham Rd, Saint Leonards-on-Sea TN38 9NS, United Kingdom*
[4]*Institut für Kernphysik, Max-von-Laue-Str. 1, 60438 Frankfurt, Germany*

(Received 6 May 2016; accepted 3 August 2016; published online 15 August 2016)

We perform wide-field time-correlated single photon counting-based fluorescence lifetime imaging (FLIM) with a crossed delay line anode image intensifier, where the pulse propagation time yields the photon position. This microchannel plate-based detector was read out with conventional fast timing electronics and mounted on a fluorescence microscope with total internal reflection (TIR) illumination. The picosecond time resolution of this detection system combines low illumination intensity of microwatts with wide-field data collection. This is ideal for fluorescence lifetime imaging of cell membranes using TIR. We show that fluorescence lifetime images of living HeLa cells stained with membrane dye di-4-ANEPPDHQ exhibit a reduced lifetime near the coverslip in TIR compared to epifluorescence FLIM. [http://dx.doi.org/10.1063/1.4961054]

Single photon detection and timing capabilities are important in a number of fields such as fluorescence spectroscopy and microscopy, lidar, optical tomography, and quantum cryptography.[1–4] Time-correlated single photon counting (TCSPC), in particular, is a precise, reliable, and mature technique to time photon arrival. Its widespread use is due to advantages afforded by its digital nature and includes a high dynamic range, high sensitivity, linearity, well-defined Poisson statistics, and easy visualization of photon arrival time data.[5]

TCSPC as a method to measure and map fluorescence decay times in fluorescence lifetime imaging microscopy (FLIM) has been reported to have the highest signal-to-noise ratio of the standard time-resolved imaging methods and is the most accurate method to detect Förster Resonance Energy Transfer (FRET).[1] It is independent of excitation intensity variations where the number of detected photons varies, but their arrival time does not. It is also independent of the fluorophore concentration, which is difficult to control in cells and tissues. TCSPC FLIM is often implemented in a scanning system, where a laser beam is scanned over the image and each photon is timed individually in each pixel of the image using a point detector. Although scanning TCSPC is a well-established technique with the benefit of optical sectioning and suppression of laterally scattered light, some fluorescence microscopy methods employ cameras. To perform single photon sensitive, picosecond resolution FLIM with these methods, a position-sensitive single photon detector with picosecond time resolution is needed.

Alternative camera-based FLIM approaches are time-gating and frequency-domain methods. The latest frequency-domain FLIM cameras are based on solid state CCD/CMOS detectors,[6,7] without an image intensifier, which avoid spatial resolution degradation and time lag artifacts due to the phosphor.[8,9] These are suitable for sufficiently bright samples so that modulation is practical,[10] where they work well with an appropriate calibration up to frame rates of ~20 fps and a time resolution down to ~100 ps.[9] For low light levels, e.g., for single molecule imaging, or low excitation intensities[11] photon counting approaches are preferable.[10]

Wide-field TCSPC requires the position of the arriving photon to be measured and recorded at the same time as the arrival time. Traditionally, microchannel plate (MCP) detectors have been used for timing photon arrival with precision of few tens of picoseconds. To also record the position, different read-out anode architectures have been developed,[12–14] where the position can be determined either from the charge division or the signal propagation time in the anode. A one-dimensional delay line anode was used on the New Horizons spacecraft for UV spectroscopy of Pluto's atmosphere,[15] and two-dimensional delay lines and quadrant anodes with bespoke read-out electronics have been used for FLIM.[11,16,17]

In this work, we have combined an MCP detector with a delay line[18] position sensitive anode and conventional fast electronics originally designed for TCSPC. This system offers picosecond time resolution and fast image acquisition for wide-field FLIM. We employ this detector for objective-based total internal reflection (TIR) microscopy, where the excitation light is reflected back from the coverslip, and the sample is excited by an evanescent wave only near (up to ~100 nm) the coverslip. We apply this system to FLIM of membrane dye di-4-ANEPPDHQ in living HeLa cells.

The 40 mm double MCP detector (Photek, UK) used in this work has an electron gain of 1×10^7, 13% quantum efficiency at 500 nm, and dark count rate of 50 counts/s/cm^2. The detector was combined with a 4-channel delay line read-out anode structure (DLD40, Roentdek, Germany). The delay line

a)Author to whom correspondence should be addressed. Electronic mail: klaus.suhling@kcl.ac.uk

is located outside the tube and coupled capacitively to a resistive anode inside the tube using the image charge technique, see Fig. 1.[19,20]

The output signal from the MCP before the anode (time channel) was amplified with a 37 dB inverting amplifier (Becker & Hickl, Germany) and input to a SPC-150 TCSPC module (Becker & Hickl, Germany). The stop signal for this channel was obtained from the laser, and the timing done in the conventional way.[5] The delay line output signals (X0, X1, Y0, and Y1) were connected to special constant fraction discriminators (CFDs) and amplifiers optimised for slow pulse rise times (Roentdek, Germany) and then connected to two SPC-150 TCSPC modules (Becker & Hickl, Germany), one for X and one for Y. X1 and Y1 signals were connected to the signal inputs, and the stop signals were obtained from X0 and Y0 after passing through a 10 m delay cable. This setup measures the propagation time difference of the signal along the delay line, Δt_x and Δt_y, and thus the photon event location. See Fig. 1 for a schematic diagram of the signal connections. Data were collected with SPCM instrument control software (Becker & Hickl, Germany).

A schematic diagram of the setup, built on a Nikon Eclipse TE2000-U microscope, is shown in Fig. 2. A Horiba DeltaDiode picosecond diode laser with 485 nm head (DD-485L) was used for excitation at 10 MHz repetition rate. In the illumination path, a mirror and a lens were mounted on a micrometer stage, which allows the illumination to be switched between wide-field and TIR illumination. A 475/28 filter was inserted in front of the laser, and neutral density filters were used in the excitation path to adjust the fluorescence count rate to $\sim 10^5$ Hz. The sample was imaged with a 60× NA1.49 TIRF oil immersion objective (Nikon, UK). The excitation and emission light was separated with a 500 nm dichroic mirror, and a 515 nm long-pass emission filter was placed in the emission path. The microscope internal magnification was set to 1.5, and a relay lens (F = 1/1.2, Canon, Japan) placed between the microscope image port and the detector provided additional magnification of 3.7.

HeLa cells were stained with polarity sensitive membrane dye di-4-ANEPPDHQ according to a protocol by

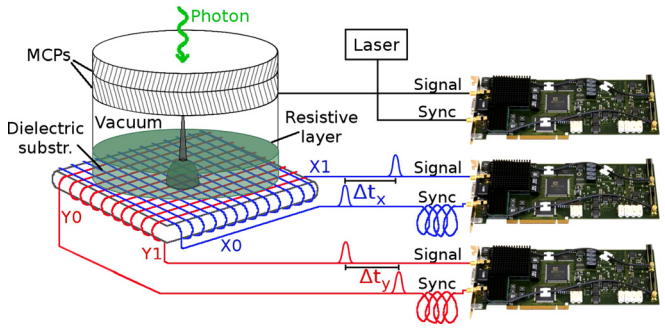

FIG. 1. Schematic diagram of the detector and its readout scheme. The delay line anode is mounted outside the MCP tube, and the charge is read out with an image charge technique.[19,20] The time signal from the MCP was connected to a TCSPC timing module signal input, and the sync (stop) signal was obtained from the excitation laser. The position signals, X1 and Y1, were connected to TCSPC timing module signal inputs, and the stop signals were obtained from the other ends of the position signals, X0 and Y0, after propagating through a 10 m delay cable. All signals were amplified before input to TCSPC timing modules.

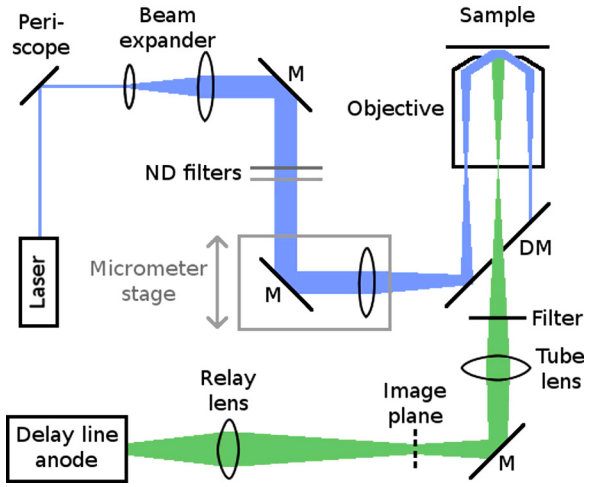

FIG. 2. Schematic diagram of the TIR FLIM setup. A picosecond pulsed UV laser was used for excitation. The beam was expanded and the intensity controlled with neutral density (ND) filters. A mirror (M) and focusing lens mounted on a micrometer stage allowed the excitation to be changed between TIR and wide-field modes. The fluorescence from the sample was collected through a dichroic mirror (DM). The image formed in the microscope image plane was magnified and focused onto the delay line anode detector with a relay lens.

Owen *et al.*[21] Cells were incubated at 37 °C-5% CO_2 with DMEM (Gibco), in 300 μl 8-well plates with coverslip bottoms (ibidi, Germany). Before staining, the medium was changed to FluoroBrite DMEM (Gibco). A 5 mM di-4-ANEPPDHQ (Molecular Probes) stock solution in DMSO (Sigma) was pre-diluted to 1/10 in de-ionised water. 3 μl of this diluted dye solution was added to the culture medium, giving a final dye concentration of 5 μM. The cells were incubated for ~12 h prior to imaging.

For instrument response function (IRF) measurement, NaI (Acros chemicals) was added to fluorescein sodium salt (Sigma) solution until the solution was saturated,[22] and a drop was placed on a multiwell plate for imaging.

Data were recorded in first-in first-out (FIFO, Parameter-Tag) mode, where each SPC-150 card writes a data file with two time stamps for each photon: microtime (time since the last excitation pulse) and macrotime (time since the start of the experiment). The three output files were combined with a program written in C by finding events that were found in the same macrotime window, corresponding to the time between laser pulses, in all three input files. The result file then only has photon events which were detected in all three (x, y, and t) channels.[5] Due to the broad pulse height distribution of the MCP, and ringing in the pulse shape caused by the delay line structure, not all events are detected in all three channels.

The 100 ns detection window was divided into 512 bins (pixels) for the x, y, and t channels, thus yielding a calibration of 0.1953 ns/channel. The lifetime images were created by placing all photons into this xyt data cube and writing the data into an .ics image file with a program written in C, fitting the time decay in each pixel of the image with Tri2 software,[23] encoding the lifetime in a pseudocolor scale (blue for short lifetimes and red for long lifetimes), and weighting the image by the fluorescence intensity image.

Fig. 3 shows TCSPC FLIM images of living HeLa cells acquired with the delay line anode detector. The measured intensity shows the cell membrane only under TIR illumination (Fig. 3(a)), while the whole cell is visible under wide-field illumination (Fig. 3(b)). The lifetime is also shortened under TIR illumination (Fig. 3(c)) compared to wide-field illumination (Fig. 3(d)); one contributory factor here is the proximity of the glass coverslip which changes the refractive index and consequently the fluorescence lifetime.[24] The lifetime variations within the images are caused by the membrane order which the dye is sensitive to; a higher membrane order causes a longer fluorescence lifetime.[21] In Fig. 3(d), the ordered membrane at cell edges shows a longer lifetime than in the centre where there are contributions from both ordered and disordered membranes. In addition, there is an alignment artefact: the longer lifetime towards the centre in Fig. 3(c) is caused by non-perfect TIR illumination. Fig. 3(f) shows the IRF and the fluorescence decays in a small area in Figs. 3(c) and 3(d). The IRF full width at half maximum (FWHM) is 315 ps.

The total TIR image data acquisition time was 93 s, with total of 7.9 million accepted photon events and count rate of 85 kHz. The wide-field image acquisition time was 86 s, with 7 million accepted photon events and count rate of 81 kHz. The event acceptance rate was 84% for the time channel and 74% and 77% for the position channels.

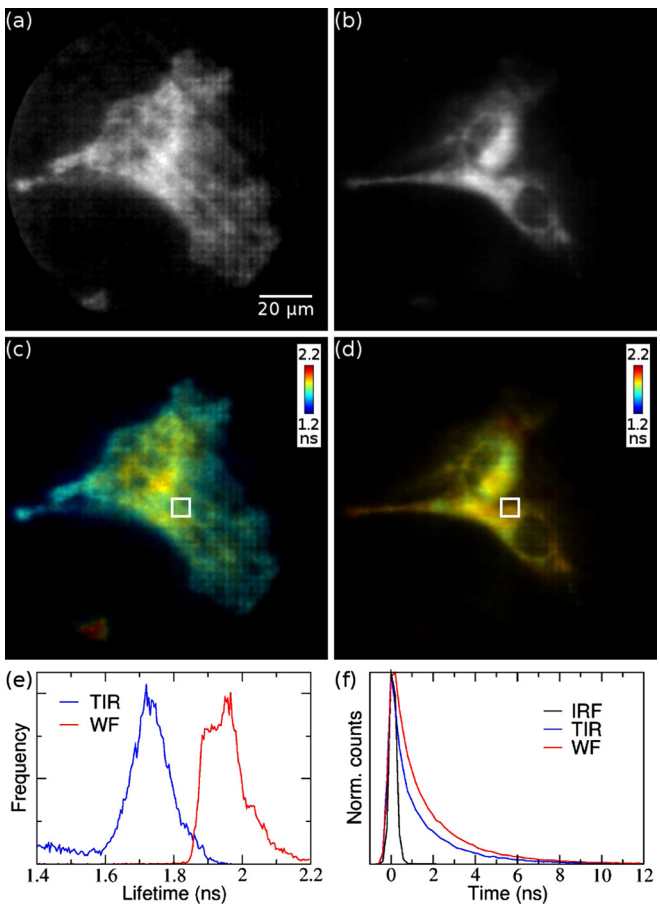

FIG. 3. TCSPC images of living HeLa cells acquired with the delay line detector. The measured intensity shows the cell membrane only under TIR illumination (a), and the lifetime is shorter (c), while the whole cell is visible under wide-field illumination (b) and the lifetime is longer (d). (e) Histogram of the individual pixel lifetimes in (c) and (d). (f) Fluorescence decays in the area indicated by a white rectangle in (c) and (d). The instrument response function, measured with quenched fluorescein solution, has a FWHM of 315 ps.

The lateral spatial resolution of the detector achieved in these experiments is ~350 μm. The 40 mm diameter active area was divided into 370 pixels, corresponding to 108 μm pixel size in the detector and 332.8 nm pixel size in the sample plane, which allows a field of view of ~123 μm diameter to be imaged. It could be possible to improve temporal and spatial resolution of the detector by optimising the CFDs which are crucial to achieve the highest resolution.[25] Optimisation of the electronics would also eliminate the horizontal and vertical stripes in the images.

A distinctive advantage of wide-field TCSPC is extremely low, uniformly distributed illumination intensity. In these experiments, ~1 μW excitation power was distributed uniformly over the field of view, yielding a maximum power of ~6.6 mW/cm^2. Averaged over the entire image area, TCSPC scanning techniques use similarly low power, but this power is concentrated in the focal spot where it reaches local intensity in the order of 10–100 W/cm^2.

The position of the detected photon in the delay line anode detector is obtained by the signal propagation time of the pulse along the delay line, so the spatial localisation is achieved by arrival timing of electronic pulses. We show here that arrival timing can be carried out with conventional TCSPC electronics, by simply connecting the delay line output, with an appropriate pulse shaping and timing CFD and pre-amplifier, to the TCSPC timing board. Converting the localisation problem to a timing problem eliminates the need for dedicated charge amplitude measurement electronics, as in position sensitive detectors employing charge division approaches.[11,16,17,20] Moreover, picosecond photon timing capabilities of the MCP combined with fast timing electronics allow IRF widths of a few hundred picoseconds to be achieved, ideal for nanosecond fluorescence lifetime measurements.

The data collection window of this 40 mm diameter detector is limited by the delay line length to 100 ns, which restricts the excitation repetition rate to 10 MHz. Only one photon per excitation period can be timed, and considering pile-up restrictions the count rate of our detector is limited to 10^5 Hz. A different timing setup allowing a pulse propagation time check would allow the detector to run in pile-up inspector mode, rejecting multiple photon events in one excitation cycle, rather than just counting the first of the two (or more) photons. This feature would eliminate pile-up bias of the decay and allow photon count rates of 37% of the excitation rate[26]—up to 3.7 MHz with the current detector's 100 ns delay line. Moreover, advanced read-out techniques, such as the hexanode comprising three crossed delay lines,[27] would allow double hits to be processed if they are separated in space and time. Note that the image charge method[19,20] used in this work allows the read-out anode to be changed easily.

CMOS cameras, which can now reach MHz frame rates, can be used in combination with MCPs for microsecond TCSPC FLIM imaging,[28,29] but conventional CMOS cameras do not reach ps time resolution which is essential for fluorescence decay measurements.

Picosecond wide-field TCSPC as described here is implemented with conventional TCSPC timing electronics, where the pulse transit time yields the photon position. This approach is ideal for TIR FLIM microscopy and is well suited for other specialised illumination microscopy techniques typically employing cameras, such as supercritical angle fluorescence microscopy or light sheet microscopy. It would also enable FLIM for camera-based super-resolution fluorescence microscopy techniques relying on single fluorophore localisation and could potentially be combined with parallelized stimulated detection[30] for low-power background-free super-resolution by TCSPC-based lifetime analysis.[31] Wide-field data collection can also combine single-particle tracking measurements with lifetime measurements,[32] while the microwatt illumination intensity, distributed uniformly over the field of view, is beneficial for long term observation of living cells.[11]

Funding from UK's BBSRC Sparking Impact scheme is gratefully acknowledged. The authors declare no conflict of interest.

[1]K. Suhling, L. M. Hirvonen, J. A. Levitt, P.-H. Chung, C. Tregidgo, A. Le Marois, D. A. Rusakov, K. Zheng, S. Ameer-Beg, S. Poland, S. Coelho, R. Henderson, and N. Krstajic, Med Photonics **27**, 3 (2015).
[2]*Advanced Time-Correlated Single Photon Counting Applications*, edited by W. Becker (Springer International Publishing, Switzerland, 2015).
[3]G. S. Buller and R. J. Collins, Meas. Sci. Technol. **21**, 012002 (2010).
[4]R. H. Hadfield, Nat. Photonics **3**, 696 (2009).
[5]W. Becker, *Advanced Time-Correlated Single Photon Counting Techniques* (Springer, Berlin, Heidelberg, 2005).
[6]A. Esposito, T. Oggier, H. Gerritsen, F. Lustenberger, and F. Wouters, Opt. Express **13**, 9812 (2005).
[7]M. Raspe, K. M. Kedziora, B. van den Broek, Q. Zhao, S. de Jong, J. Herz, M. Mastop, J. Goedhart, T. W. Gadella, I. T. Young, and K. Jalink, Nat. Methods **13**, 501 (2016).
[8]Q. Zhao, B. Schelen, R. Schouten, R. van den Oever, R. Leenen, H. van Kuijk, I. Peters, F. Polderdijk, J. Bosiers, M. Raspe, K. Jalink, J. G. S. de Jong, B. van Geest, K. Stoop, and I. T. Young, J. Biomed. Opt. **17**, 126020 (2012).
[9]H. Chen, G. Holst, and E. Gratton, Microsc. Res. Tech. **78**, 1075 (2015).
[10]E. Gratton, S. Breusegem, J. Sutin, Q. Ruan, and N. Barry, J. Biomed. Opt. **8**, 381 (2003).
[11]Z. Petrášek, H.-J. Eckert, and K. Kemnitz, Photosynth. Res. **102**, 157 (2009).
[12]J. S. Lapington, Nucl. Instrum. Methods Phys. Res., Sect. A **525**, 361 (2004).
[13]X. Michalet, R. A. Colyer, G. Scalia, A. Ingargiola, R. Lin, J. E. Millaud, S. Weiss, O. H. Siegmund, A. S. Tremsin, J. V. Vallerga, A. Cheng, M. Levi, D. Aharoni, K. Arisaka, F. Villa, F. Guerrieri, F. Panzeri, I. Rech, A. Gulinatti, F. Zappa, M. Ghioni, and S. Cova, Philos. Trans. R. Soc. B **368**, 20120035 (2013).
[14]J. Vallerga, J. McPhate, A. Tremsin, and O. Siegmund, Astrophys. Space Sci. **320**, 247 (2009).
[15]S. A. Stern, D. C. Slater, J. Scherrer, J. Stone, G. Dirks, M. Versteeg, M. Davis, G. R. Gladstone, J. W. Parker, L. A. Young, and O. H. W. Siegmund, Space Sci. Rev. **140**, 155 (2008).
[16]V. Emiliani, D. Sanvitto, M. Tramier, T. Piolot, Z. Petrášek, K. Kemnitz, C. Durieux, and M. Coppey-Moisan, Appl. Phys. Lett. **83**, 2471 (2003).
[17]G. Giraud, H. Schulze, T. T. Bachmann, C. J. Campbell, A. R. Mount, P. Ghazal, M. R. Khondoker, A. J. Ross, S. W. J. Ember, I. Ciani, C. Tlili, A. J. Walton, J. G. Terry, and J. Crain, Int. J. Mol. Sci. **10**, 1930 (2009).
[18]O. H. W. Siegmund, M. Lampton, R. Raffanti, and W. Herrick, Nucl. Instrum. Methods Phys. Res., Sect. A **310**, 311 (1991).
[19]J. Milnes, J. S. Lapington, O. Jagutzki, and J. Howorth, Nucl. Instrum. Methods Phys. Res., Sect. A **604**, 218 (2009).
[20]O. Jagutzki, J. S. Lapington, L. B. C. Worth, U. Spillman, V. Mergel, and H. Schmidt-Böcking, Nucl. Instrum. Methods Phys. Res., Sect. A **477**, 256 (2002).
[21]D. M. Owen, C. Rentero, A. Magenau, A. Abu-Siniyeh, and K. Gaus, Nat. Protoc. **7**, 24 (2012).
[22]M. Liu, M. Jia, H. Pan, L. Li, M. Chang, H. Ren, F. Argoul, S. Zhang, and J. Xu, Appl. Spectrosc. **68**, 577 (2014).
[23]P. R. Barber, S. M. Ameer-Beg, J. Gilbey, L. M. Carlin, M. Keppler, T. C. Ng, and B. Vojnovic, J. R. Soc., Interface **6**, S93 (2009).
[24]C. Tregidgo, J. A. Levitt, and K. Suhling, J. Biomed. Opt. **13**, 031218 (2008).
[25]J. V. Vallerga and J. B. McPhate, Proc SPIE **4139**, 34 (2000).
[26]C. C. Davis and T. A. King, J. Phys. A: Gen. Phys. **3**, 101 (1970).
[27]O. Jagutzki, A. Cerezo, A. Czasch, R. Dörner, M. Hattaß, M. Huang, V. Mergel, U. Spillmann, K. Ullmann-Pfleger, T. Weber, H. Schmidt-Böcking, and G. Smith, IEEE Nucl. Sci. Symp. Conf. Rec. **2**, 850 (2001).
[28]L. M. Hirvonen, Z. Petrášek, A. Beeby, and K. Suhling, New J. Phys. **17**, 023032 (2015).
[29]L. M. Hirvonen, F. Festy, and K. Suhling, Opt. Lett. **39**, 5602 (2014).
[30]A. Chmyrov, J. Keller, T. Grotjohann, M. Ratz, E. d'Este, S. Jakobs, C. Eggeling, and S. W. Hell, Nat. Methods **10**, 737 (2013).
[31]L. Lanzano, I. Coto Hernandez, M. Castello, E. Gratton, A. Diaspro, and G. Vicidomini, Nat. Commun. **6**, 6701 (2015).
[32]X. Michalet, R. Colyer, J. Antelman, O. Siegmund, A. Tremsin, J. Vallerga, and S. Weiss, Curr. Pharm. Biotechnol. **10**, 543 (2009).